Critical Parameters and Saturated Density of Trifluoroiodomethane (CF_3I)

Yuan-Yuan Duan,* Lin Shi, Ming-Shan Zhu, and Li-Zhong Han

Department of Thermal Engineering, Tsinghua University, Beijing, 100084, People's Republic of China

The vapor−liquid coexistence curve of trifluoroiodomethane (CF_3I) was measured by visual observation of the meniscus disappearance in an optical cell. Thirty-two saturated density data points were obtained along the vapor−liquid coexistence curve between 384.5 and 2024.9 kg·m^{-3} in the temperature range from 301.02 K to the critical temperature. The experimental uncertainties in temperature and density were estimated to be within ±10 mK and ±0.5%, respectively. Measurements near the critical point were used to determine the critical temperature T_c = 396.44 ± 0.01 K and the critical density ρ_c = 868 ± 3 kg·m^{-3} for trifluoroiodomethane (CF_3I) on the basis of the meniscus disappearing level as well as the intensity of the critical opalescence. The critical pressure p_c = 3.953 ± 0.005 MPa was extrapolated from the existing vapor pressure equation proposed previously (Duan, Y. Y.; Zhu, M. S.; Han, L. Z. *Fluid Phase Equilib.* **1996**, *121*, 227−234) using the present T_c value. The critical exponent, β, was also determined, and correlations of the saturated liquid and saturated vapor densities of CF_3I were developed.

Introduction

CFC-12 is widely used in numerous applications as the traditional refrigerant. Alternatives to CFC-12 must be developed that are environmentally acceptable and can be used in high-capacity, high-efficiency applications. HFC-134a has been widely used as a replacement for CFC-12, especially in the USA, Japan, the U.K., and France, but it requires physical retrofitting of equipment and is not miscible with mineral oil. It also has a higher global warming potential (GWP) value. Hydrocarbons are considered to be another promising alternative, especially in Germany, even though they are flammable. CF_3I has been found to be non-ozone, depleting, miscible with mineral oil, and compatible with refrigeration system materials. It also has an extremely low GWP value and very low acute toxicity. Therefore, CF_3I is also being considered as a promising alternative, especially as a component in mixtures, to replace CFC-12 (Lankford and Nimitz, 1993; Zhao et al., 1995). We have measured some of the thermophysical properties of CF_3I, i.e. vapor pressure (Duan et al., 1996), *PVT* (Duan et al., 1997a), speed of sound (Duan et al., 1997b), and thermal conductivity (Duan et al., 1997c). Unfortunately, reliable critical parameters and saturated density property data for CF_3I are still limited. The critical parameters, i.e. critical temperature T_c, critical density ρ_c, and critical pressure p_c, are important not only for understanding the thermodynamic state of the surface of fluids but also for developing the correlations and predictive methods for the thermophysical properties using the principle of corresponding states. In the present study, measurements of the vapor−liquid coexistence curve for CF_3I have been performed and the critical parameters and saturated density for CF_3I have been determined precisely.

Experimental Section

An experimental apparatus, schematically shown in Figure 1, was constructed for determining the critical parameters of fluids. The experimental cell was an optical cell with two Pyrex windows (15 mm in thickness) used to observe the meniscus of the inner sample and is shown in Figure 2. The body of the experimental cell was made of 1Cr18Ni9Ti stainless steel. The inner volume of the cell, determined by calibration with distilled, deionized water, was 9.784 ± 0.003 cm^3 at 15 °C. The experimental cell was fixed in an empty stainless container with two Pyrex

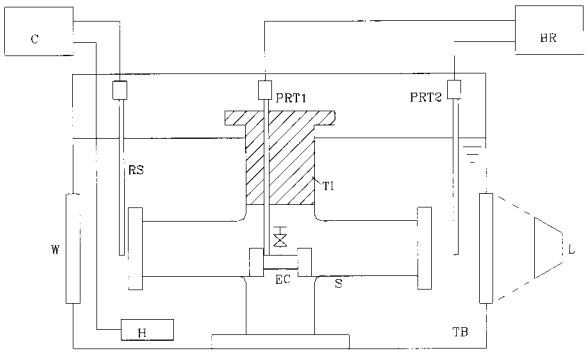

Figure 1. Critical parameters and saturated density measurement apparatus: EC, experimental cell; TB, thermostated bath; S, shell; W, window; L, light; TI, thermal insulation; H, heater; RS, thermal-sensitive resistance sensor; PRT1, PRT2, platinum resistance thermometer; C, controller; BR, automatic thermometer bridge.

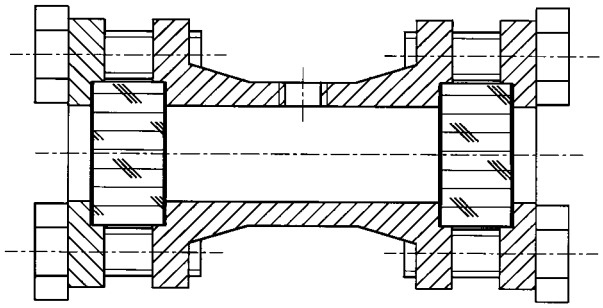

Figure 2. Experimental cell for observing sample meniscus.

* To whom correspondence should be addressed. E-mail: yyduan@te.tsinghua.edu.cn.

10.1021/je980251b CCC: $18.00
Published on Web 03/19/1999

Table 1. Experimental Results for Saturated Densities of CF_3I[a]

T/K	ρ/(kg·m^{-3})	T/K	ρ/(kg·m^{-3})
301.022	2024.9	390.295	1229.9
307.132	1992.0	392.617	1173.0
313.094	1958.2	394.264	1124.9
319.751	1917.1	395.296	1070.5
319.933	1915.5	395.845	1020.3
322.082	1902.8	396.167	983.4*
326.031	1878.5	396.424	920.7*
331.485	1843.5	396.439	894.5*
334.742	1822.5	396.446	872.6*
339.804	1793.6	396.438	865.7*
340.831	1781.2	396.442	857.2*
344.140	1758.3	396.265	751.3*
355.192	1676.7	395.860	695.7
368.585	1552.1	394.563	607.8
378.134	1438.8	390.968	499.6
386.590	1305.3	383.843	384.5

[a] Asterisk indicates critical opalescence was observed.

windows, and the container was assembled and immersed in a thermostated bath. Although the equilibrium time between the sample fluid and the heat transfer medium was longer, the temperature stability was improved. The temperature of the thermostated bath could be varied from 233 to 453 K. The temperature instability in the bath was less than ±5 mK during 8 h. It can be used to measure vapor pressure, *PVT* properties, critical parameters, etc. Silicone oil, distilled deionized water, or alcohol was used as the fluid in the bath, depending on the temperature range.

A platinum resistance thermometer, installed near the experimental cell in the stainless container, was used for temperature measurements. Another platinum resistance thermometer was installed in the thermostated bath to detect the temperature fluctuations. The temperature measurement system included the platinum resistance thermometers (5187SA) with an uncertainty of ±2 mK, a precision Tinsley thermometer bridge (5840D), with an accuracy within ±1 mK, a select switch (5840CS/6T), and a personal computer. The overall temperature uncertainty for the bath and the temperature measurement system was less than ±10 mK. The temperatures were determined on the ITS-90 throughout the present paper.

The density of the sample in the experimental cell was calculated from the mass of the sample, which was weighted on a precision chemical balance (Shanghai, TG31), and the inner volume of the vessel. The saturation temperature along the vapor−liquid coexistence curve for a specified density was determined by observing the meniscus disappearance in the experimental cell. After each saturation temperature measurement, part of the sample in the experimental cell was carefully discharged to change the sample density in the experimental cell. The mass of the sample was measured for the determination of the new density; then the saturation temperature was measured again.

The CF_3I sample was provided by Pacific Scientific. The manufacture stated that the CF_3I sample purity of was 99.95 mass % with 3−4 ppm of water. The sample was used without further purification.

Results and Discussion

Results. Thirty-two saturated density data points for CF_3I were obtained along the vapor−liquid coexistence curve from 301 K to the critical temperature corresponding to densities between 384.5 and 2024.9 kg·m^{-3}. The experimental results are given in Table 1. The experimental uncertainties in temperature and density were estimated to be within ±10 mK and ±0.5%, respectively.

The meniscus for 23 densities between 920.7 and 2024.9 kg·m^{-3} ascended with increasing temperature and disappeared at the top of the experimental cell, while it descended and disappeared at the bottom of the experimental cell for five densities between 384.5 and 751.3 kg·m^{-3}. From these appearances, it can be determined that the density in the experimental cell corresponded to the saturated liquid density or saturated vapor density. The meniscus disappeared without reaching either the top or bottom of the experimental cell at four densities between 857.2 and 894.5 kg·m^{-3}. The critical opalescence was observed at seven measurements in densities between 751.3 and 983.4 kg·m^{-3} which correspond to temperatures above 0.3 K below the critical temperature; these measurements are indicated with an asterisk in Table 1.

Critical Parameters. At the critical point, the meniscus disappears at the center of the experimental cell and the critical opalescence is most intense and equal in both the vapor and liquid phases. By this definition, it is possible to distinguish whether the sample density in the experimental cell corresponds to the saturated liquid density or saturated vapor density. For the two densities of 865.7 and 872.6 kg·m^{-3}, the meniscus level was unchanged at the center of the experimental cell with increasing temperature and the most intense opalescence was observed in the seven measurements identified as the critical opalescence. Careful examination showed that at the density of 865.7 kg·m^{-3}, the critical opalescence in the liquid phase was a little more intense than in the vapor phase, while the critical opalescence in the vapor phase was a little more intense than in the liquid phase at a density of 872.6 kg·m^{-3}. Therefore the critical density of CF_3I is between 865.7 and 872.6 kg·m^{-3}.

Considering the meniscus behavior near the critical point and the uncertainty of the present density measurements, the critical density of CF_3I was determined to be

$$\rho_c = 868 \pm 3 \text{ kg·m}^{-3} \quad (1)$$

The critical temperature of pure fluids is defined as the maximum temperature along the vapor−liquid coexistence curve, and it is the saturation temperature corresponding to the critical density. The critical temperature can be easily determined, because the shape of the top of the vapor−liquid coexistence curve is almost flat in the vicinity of the critical point. On the basis of the experimental results listed in Table 1, the critical temperature of CF_3I was determined to be

$$T_c = 396.44 \pm 0.01 \text{ K} \quad (2)$$

Although the saturation temperatures for the densities of 857.2 and 872.6 kg·m^{-3} were higher than T_c by 2 mK and 6 mK, these differences are within the uncertainty of the present temperature measurements.

The critical pressure p_c could not be determined directly from this experimental apparatus. In the present work, the critical pressure of CF_3I was extrapolated from the vapor pressure equation (Duan et al., 1996) with the aid of the T_c value given in eq 2. The uncertainty of the critical pressure depends upon the uncertainty of the critical temperature and the accuracy of the vapor pressure equation. The critical pressure of CF_3I was calculated to be

$$r_c = 3.953 \pm 0.005 \text{ MPa} \quad (3)$$

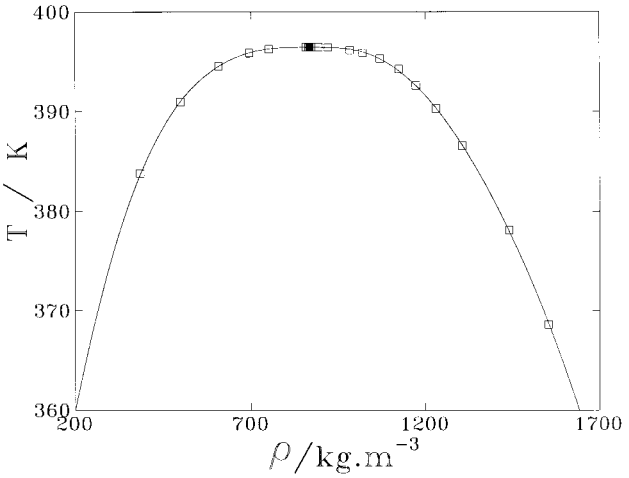

Figure 3. Vapor−liquid coexistence curve in the critical region of CF_3I: (□) experimental data; (■) critical point.

Table 2. Critical Parameters of CF_3I

ref	T_c/K	ρ_c/(kg·m^{-3})	p_c/MPa
Sladkov and Bogacheva, 1991	395.15	871	4.04
UNEP, 1995	395.05		4.04
Duan et al., 1996	395.05		3.8617
present work 1998	396.44 ± 0.01	868 ± 3	3.953 ± 0.005

Table 2 compares the present critical parameters with those determined by other authors. The present ρ_c value agrees well with the value of Sladkov and Bogacheva (1991), but the present T_c value is higher than that of Sladkov and Bogacheva (1991) and that of UNEP (1995) by 1.29 K and 1.39 K, respectively. The present p_c value is lower than those of Sladkov and Bogacheva and UNEP. The p_c value of Duan et al. (1996), determined by extrapolation of the vapor pressure equation using the T_c value of UNEP, is lower than the present p_c value.

Discussion. The critical exponent, β, is important for modeling the vapor−liquid coexistence curve in the critical region by means of the following power law representation:

$$(\rho' - \rho'')/2\rho_c = B[(T_c - T)/T_c]^{\beta} \quad (4)$$

where ρ', ρ'', T, ρ_c, T_c, and B denote saturated liquid density, saturated vapor density, temperature, critical density, critical temperature, and critical amplitude, respectively. The correlation of the vapor−liquid coexistence curve was formulated using the Wagner expansion (Levelt Sengers and Sengers, 1981):

$$\Delta\rho^* = D_0|\Delta T^*|^{(1-\alpha)} + D_1|\Delta T^*| + D_2|\Delta T^*|^{(1-\alpha+\Delta_1)} \pm B_0|\Delta T^*|^{\beta} \pm B_1|\Delta T^*|^{(\beta+\Delta_1)} \quad (5)$$

where $\Delta\rho^* = (\rho - \rho_c)/\rho_c$ and $\Delta T^* = (T - T_c)/T_c$; the exponents are $\alpha = 0.1085$, $\beta = 0.325$, and $\Delta_1 = 0.50$. The coefficients $D_0 = -12.617\,79$, $D_1 = 21.110\,48$, $D_2 = -10.436\,21$, $B_1 = 1.572\,056$, and $B_2 = 0.760\,6325$ were determined by a least-squares fit using the experimental data in the reduced temperature range $T/T_c > 0.93$ except for the four data points between 857.2 and 894.5 kg·m^{-3} around the critical point. The plus sign (+) and the minus sign (−) of the fourth and fifth terms in eq 5 correspond to saturated liquid and vapor, respectively. The saturation curves calculated from eq 5 are shown in Figure 3. The correlation is effective in a range of densities from 384.5 to 1305.3 kg·m^{-3}. Figure 4, the relative deviations of the experimental data from eq 5, shows that the maximum deviation of the experimental data from eq 5 was less than 1%. Figure 5 shows a logarithmic plot in terms of the experimental data and calculated results from eq 5. Fifteen experimental data points near the critical point were used to determine the critical exponent, β, and the critical amplitude, B, with a least-squares fit. Their values are $\beta = 0.342$ and $B = 1.810$.

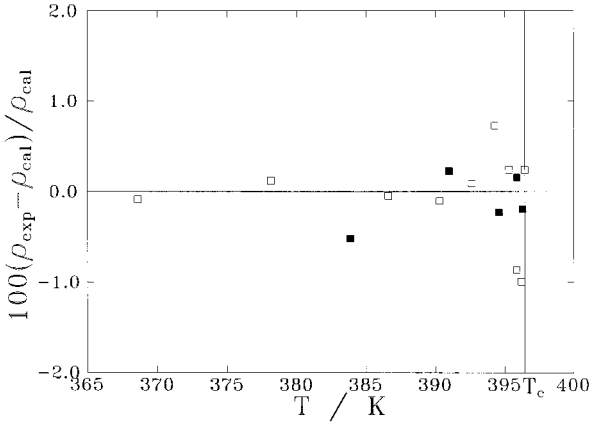

Figure 4. Density deviation of CF_3I from eq 5: (□) saturated liquid; (■) saturated vapor.

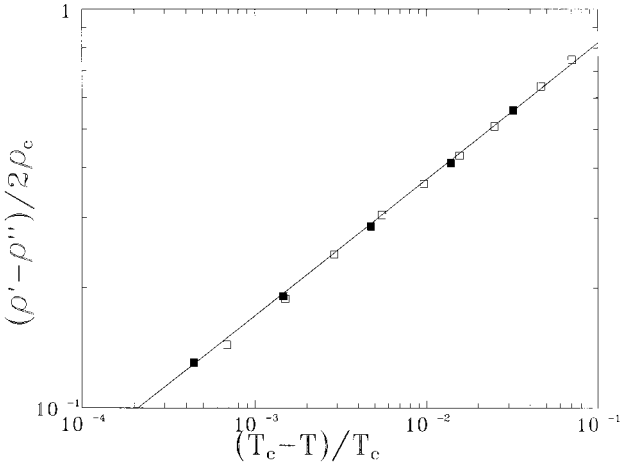

Figure 5. Critical exponent and amplitude of CF_3I: (□) saturated liquid ; (■) saturated vapor.

Table 3. Coefficients for Equation 6

	b_1	b_2	b_3	b_4
saturated liquid	1.401 532	0.809 2603	0.594 6375	−0.399 1380
saturated vapor	−1.542 282	−1.149 425	2.020 176	−0.377 6717

Saturated Density Correlations. There are only three points of saturated liquid density data available for CF_3I before the present work (Emeleus and Wood, 1948; Nodiff and Grosse, 1953) and no available experimental data for the saturated vapor density. The experimental *PVT* properties and an equation of state for gaseous CF_3I was reported previously by Duan et al. (1997a). The maximum density of the experimental data along each isotherm was very close to the corresponding saturated vapor density for temperatures below 353 K. Therefore the saturated vapor density of CF_3I can be calculated from the previously determined equation of state and the vapor pressure correlation (Duan et al., 1996) at temperatures less than 353 K. The updated experimental data and saturated vapor densities extrapolated from the CF_3I *PVT* measurements were used to correlate the saturated liquid and vapor

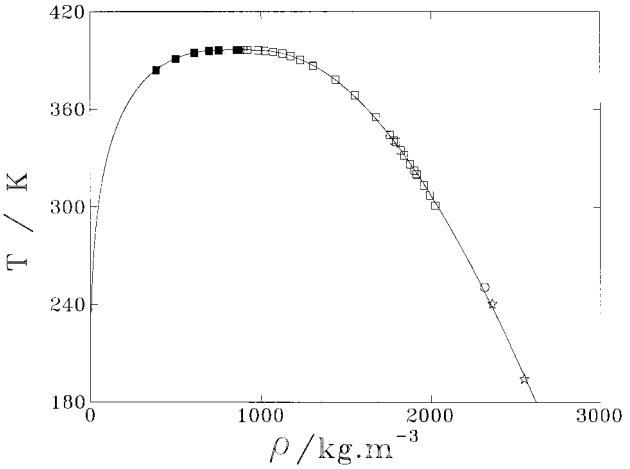

Figure 6. Vapor−liquid coexistence curve calculated from eq 6 and experimental saturated density data of CF_3I: (□) present saturated liquid density; (■) present saturated vapor density; (○) Emeleus and Wood (1948); (☆) Nodiff and Grosse (1953).

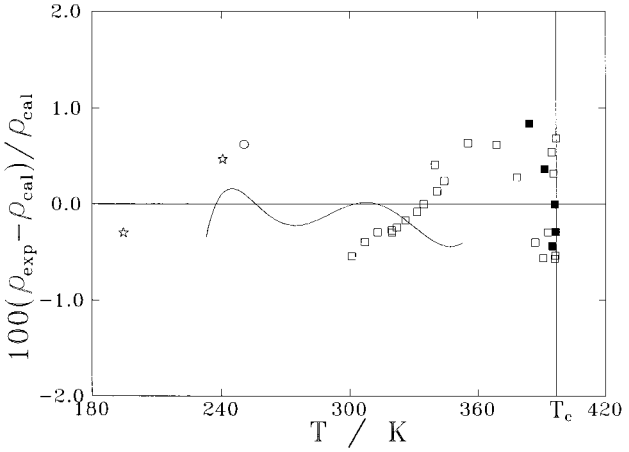

Figure 7. Relative deviations of available saturated density data from eq 6: (□) present saturated liquid density; (■) present saturated vapor density; (○) Emeleus and Wood (1948); (☆) Nodiff and Grosse (1953); (—) saturated vapor density calculated from equation of state.

densities as

$$\rho_r = 1 + b_1\tau^{\beta} + b_2\tau^{2\beta} + b_3\tau + b_4\tau^{1/\beta} \qquad (6)$$

where, $\rho_r = \rho/\rho_c$, $\rho_c = 868$ kg·m^{-3} is the critical density, $\beta = 0.325$ is the critical exponent, and b_1, b_2, b_3, and b_4 are coefficients determined by the least-squares fit, and the values for saturated liquid and saturated vapor are listed in Table 3.

The vapor−liquid coexistence curve for CF_3I calculated from eq 6 and the updated available data are shown in Figure 6. The relative deviations of the experimental data from eq 6 are shown in Figure 7, where the maximum deviation is less than 1%. Equation 6 is effective in the temperature range from 195 K to the critical point for saturated liquid and from 233 K to the critical point for saturated vapor.

Conclusion

Visual observation of the meniscus in the optical cell was used to measure the vapor−liquid coexistence curve of CF_3I and the critical parameters, and the critical exponent, β, was determined. The correlations of saturated vapor and liquid densities for CF_3I were developed on the basis of the present measurements and other available results. The correlations are able to represent the experimental results within ±1% in the temperature range from 195 K to the critical temperature for saturated liquid and from 233 K to the critical temperature for saturated vapor.

Acknowledgment

We are grateful to Dr. Nimitz of IKON Co. and the Pacific Scientific for providing the CF_3I sample.

Literature Cited

Duan, Y. Y.; Zhu, M. S.; Han, L. Z. Experimental Vapor Pressure Data and a Vapor Pressure Equation for Trifluoroiodomethane (CF_3I). *Fluid Phase Equilib.* **1996**, *121*, 227−234.

Duan, Y. Y.; Zhu, M. S.; Shi, L.; Han, L. Z. Experimental Pressure-Volume-Temperature Data and An Equation of State for Gaseous Trifluoroiodomethane (CF_3I). *Fluid Phase Equilib.* **1997a**, *131*, 233−241.

Duan Y. Y.; Sun L. Q.; Shi L.; Zhu M. S.; Han L. Z. Speed of Sound and Ideal-Gas Heat Capacity at Constant Pressure of Gaseous Trifluoroiodomethane (CF_3I). *Fluid Phase Equilib.* **1997b**, *137*, 121−131.

Duan, Y. Y.; Sun, L. Q.; Shi, L.; Zhu, M. S.; Han, L. Z. Thermal Conductivity of Gaseous Trifluoroiodomethane (CF_3I). *J. Chem. Eng. Data* **1997c**, *42*, 890−893.

Emeleus, H. J.; Wood, J. F. The Preparation and Reactions of Carbonyl and Sulphuryl Fluorides and Chlorofluorides. *J. Chem. Soc.* **1948**, 2183−2188.

Lankford, L.; Nimitz, J. A New Class of High-Performance, Environmentally Sound Refrigerants. *Proceedings of the International CFC and Halon Alternatives Conference*, Washington, DC; 1993; pp 141−149.

Levelt Sengers, J. M. H.; Sengers, J. V. *Perspectives in Statistical Physics*; Raveche, H. J., Ed.; North-Holland: Amsterdam, 1981.

Nodiff, E. A.; Grosse, A. V.; Hauptshein, M. Physical Properties of *N*-Perfluoroalkyl Halides and Dihalides and A Comparison With The Corresponding Alkyl Compounds. *J. Org. Chem.* **1953**, 235−243.

Sladkov, I. B.; Bogacheva, A. V. Critical Parameters of Mixed Carbon Halides. *Zh. Prikl. Khim.* **1991**, *64*, 2435−2437.

UNEP. 1994 Report of the refrigeration, air condition and heat pumps technical option committee; UNEP: Nairobi, 1995; p 40.

Zhao, X. Y.; Shi, L.; Zhu, M. S.; Han, L. Z. A New Generation of Long-Term Refrigerants as CFC-12 Alternatives. *Proceedings of the International CFC and Halon Alternatives Conference*, Washington, DC; 1995; pp 286−293.

Received for review October 15, 1998. Accepted January 19, 1999. This work was supported by the State Education Commission of People's Republic of China (Grant No. 9400364).

JE980251B